Nonlinear Dynamics and Applications. Vol. 13 (2006) 177 - 182

Searching for new physics scenarios at e^+e^- linear colliders with polarized beams

A. A. Pankov* and A. V. Tsytrinov†

ICTP Affiliated Centre, Pavel Sukhoi Technical University, Gomel 246746, Belarus

Four-fermion contact interactions can manifest themselves through deviations of observables from the standard model (SM) predictions. We consider a number of such nonstandard scenarios, and discuss their identification as sources of deviations in fermion-pair production processes at the International Linear Collider (ILC) with high energy $\sqrt{s} = 1\,\mathrm{TeV}$ and time-integrated luminosity $\mathcal{L}_{\mathrm{int}} = 1000\,\mathrm{fb}^{-1}$, respectively, if they were observed. The availability of initial beams longitudinal polarization is also taken into account in the analysis.

PACS numbers: 12.60.–i

Keywords: four-fermion contact interactions, fermion-pair production, linear collider

1. Introduction

New physics (NP) beyond the standard model is expected to show up at the LHC and ILC colliders either *directly* through production of new particles, or *indirectly* through *deviations* of cross sections and asymmetries from the SM predictions. The latter case is typical of interactions mediated by exchanges of heavy mass objects, such that the energy is not sufficient for their direct production. The corresponding corrections to the SM predictions are most conveniently parameterized in terms of negative powers of the characteristic large mass scales Λ, times matrix elements of effective, contactlike, Lagrangians.

The so-called *discovery reach*, i.e., the maximum value of Λ for which a deviation could be observed within the foreseeable experimental accuracy, gives an indication of the expected sensitivity of an observable to the various NP scenarios. On the other hand, in principle different NP models can cause similar deviations. Therefore, it should be interesting to assess the *identification reach* on the individual models, i.e., the maximum value of Λ for which a novel interaction not only produces observable deviations, but also can be discriminated, as the source of the observed deviations, from the other nonstandard interactions for all values of their characteristic mass scale parameters. Clearly, by definition, the identification reach is expected to be smaller than the discovery reach. Here we discuss the differential cross sections for the following processes at the ILC with both beams longitudinally polarized:

$$e^+ + e^- \to \bar{f} + f, \qquad f = e, \mu, \tau, c, b\,. \tag{1}$$

These processes can all receive corrections from the contactlike interactions considered here,

*pankov@ictp.it

†tsytrin@gstu.gomel.by

and their sensitivity is significantly enhanced by the initial e^- and e^+ polarizations [1–4]. This facility is envisaged at the planned ILC [5].

The nonstandard scenarios we consider are the following:

a) The ADD large compactified extra dimensions scenario [6–8], where only gravity can propagate in the extra spatial dimensions, and correspondingly a tower of graviton KK states is exchanged in the four-dimensional space [9, 10]. The relevant, dimension-8, effective Lagrangian can be expressed as [11]:

$$\mathcal{L}^{\mathrm{ADD}} = i\frac{4\lambda}{\Lambda_H^4} T^{\mu\nu} T_{\mu\nu}, \tag{2}$$

with $T_{\mu\nu}$ being the energy-momentum tensor of the SM particles and Λ_H a phenomenological cutoff on the summation over the KK spectrum, expected in the (multi) TeV region. Here, $\lambda = \pm 1$.

b) Gravity in TeV^{-1}–scale extra dimensions, in which also the SM gauge bosons can propagate. The relevant contactlike effective Lagrangian can be parameterized by a "compactification scale" M_C, and for one extra dimension it reads [12, 13]:

$$\begin{aligned}\mathcal{L}^{\mathrm{TeV}} &= -\frac{\pi^2}{3M_C^2}[Q_e Q_f(\bar{e}\gamma_\mu e)(\bar{f}\gamma^\mu f) \\ &+ (g_{\mathrm{L}}^e \bar{e}_{\mathrm{L}}\gamma_\mu e_{\mathrm{L}} + g_{\mathrm{R}}^e \bar{e}_{\mathrm{R}}\gamma_\mu e_{\mathrm{R}})(g_{\mathrm{L}}^f \bar{f}_{\mathrm{L}}\gamma^\mu f_{\mathrm{L}} + g_{\mathrm{R}}^f \bar{f}_{\mathrm{R}}\gamma^\mu f_{\mathrm{R}})].\end{aligned} \tag{3}$$

c) The dimension-6 four-fermion contact interactions (CI) [14, 15], with $\Lambda_{\alpha\beta}$ "compositeness" mass scales ($\alpha, \beta = \mathrm{L}, \mathrm{R}$ and $\eta_{\alpha\beta} = \pm 1, 0$):

$$\mathcal{L}^{\mathrm{CI}} = \frac{4\pi}{1+\delta_{ef}} \sum_{\alpha,\beta} \frac{\eta_{\alpha\beta}}{\Lambda_{\alpha\beta}^2} \left(\bar{e}_\alpha \gamma_\mu e_\alpha\right) \left(\bar{f}_\beta \gamma^\mu f_\beta\right). \tag{4}$$

Current experimental lower bounds on the above mass scales at the 95% C.L. are $\Lambda_H > 1.3\,\mathrm{TeV}$ and $M_C > 6.8\,\mathrm{TeV}$ [16] while, generically, those on Λs of Eq. (4) are in the range 10–15 TeV [17].

2. Discovery and identification reaches

For an extensive presentation of the analysis and a full account of the numerical results for the expected discovery and identification reaches we refer to [1]. Basically, for the polarized angular distributions, $\mathcal{O} = \mathrm{d}\sigma/\mathrm{d}\cos\theta$, we introduce the relative deviations from the SM predictions:

$$\Delta(\mathcal{O}) = \frac{\mathcal{O}(\mathrm{SM}+\mathrm{NP}) - \mathcal{O}(\mathrm{SM})}{\mathcal{O}(\mathrm{SM})} \tag{5}$$

and the corresponding χ^2:

$$\chi^2(\mathcal{O}) = \sum_{\mathrm{bins}} \left(\frac{\Delta(\mathcal{O})^{\mathrm{bin}}}{\delta\mathcal{O}^{\mathrm{bin}}}\right)^2. \tag{6}$$

Here, the angular range has been divided into ten equal-size bins, and $\delta\mathcal{O}^{\mathrm{bin}}$ denotes the expected relative uncertainty, statistical plus systematic ones, in each bin. The discovery reaches on models (2)-(4) can be assessed by assuming non-observation of deviations and,

Table 1. 95% C.L. discovery reaches (in TeV) at $\sqrt{s} = 1$ TeV and $\mathcal{L}_{\rm int} = 1000\ fb^{-1}$. Left and right entries refer to the polarization configurations $(|P^-|,|P^+|)$=(0,0) and (0.8,0.6), respectively.

Model	Process			
	$e^+e^- \to e^+e^-$	$e^+e^- \to l^+l^-$	$e^+e^- \to \bar{b}b$	$e^+e^- \to \bar{c}c$
Λ_H	8.7; 9.4	6.7; 7.0	6.7; 7.5	6.7; 7.1
Λ^{ef}_{VV}	173.6; 205.1	218.8; 244.3	185.6; 238.2	206.2; 232.3
Λ^{ef}_{AA}	109.9; 166.1	194.7; 217.9	186.; 242.7	186.4; 210.8
Λ^{ef}_{LL}	83.7; 122.8	128.3; 165.5	154.5; 175.8	131.3; 159.6
Λ^{ef}_{RR}	80.5; 122.1	123.4; 166.1	103.5; 176.9	111.8; 164.1
Λ^{ef}_{LR}	136.6; 166.8	120.5; 156.6	124.9; 170.2	92.7; 144.6
Λ^{ef}_{RL}	$\Lambda^{ee}_{RL} = \Lambda^{ee}_{LR}$	120.8; 158.3	120.1; 151.9	129.6; 151.1
M_C	27.2; 32.5	48.3; 54.2	15.6; 26.5	26.2; 30.2

accordingly, are determined by the condition $\chi^2(\mathcal{O}) < \chi^2_{\rm CL}$. Here, we take $\chi^2_{\rm CL} = 3.84$ for a 95% C.L. In Table 1 we present numerical results for an ILC with parameters as specified in the caption. The assumed reconstruction efficiencies are 100% for e^+e^- final pairs; 95% for l^+l^- events ($l = \mu, \tau$); 35% and 60% for $c\bar{c}$ and $b\bar{b}$, respectively. The major systematic uncertainties originate from uncertainties on beams polarizations and on the time-integrated luminosity, for which we have assumed $\delta P^-/P^- = \delta P^+/P^+ = 0.2\%$ and $\delta\mathcal{L}_{\rm int}/\mathcal{L}_{\rm int} = 0.5\%$, respectively. The results in Table 1 clearly show the enhancement in sensitivity to NP models allowed, at a given c.m. energy, by beams polarization. In particular, this effect is dramatic in the case of the CI models (4).

Continuing the previous χ^2-based analysis, we now assume that a deviation has been observed, for example consistent with the ADD scenario (2) with some value of Λ_H. To assess the level at which the ADD model can be identified from the other models potential sources of the deviation, we choose, for example, the AA model of Eq. (4), and introduce relative deviations:

$$\Delta(\mathcal{O}) = \frac{\mathcal{O}(\mathrm{AA}) - \mathcal{O}(\mathrm{ADD})}{\mathcal{O}(\mathrm{ADD})} \tag{7}$$

and corresponding χ^2 similar to Eq. (6). Now χ^2 is a function of λ/Λ_H^4 and $\eta/\Lambda^2_{\rm AA}$, and we can determine, in the plane of these parameters, the *confusion region* where the AA model can be considered as consistent with the ADD. At the 95% C.L., one determines such confusion region from the condition $\chi^2 < 3.84$. The contour of the confusion region identifies a maximal value of $|\lambda/\Lambda_H^4|$ (equivalently, a minimum value of Λ_H), for which the AA model can *excluded* at the 95 % C.L. for any value of $\eta/\Lambda^2_{\rm AA}$. This value, $\Lambda_H^{\rm AA}$, is the *exclusion reach* on the AA model. Fig. 1 shows an example of confusion region obtained by different polarization. This procedure can be repeated for all other interactions in Eqs. (3) and (4), to determine the individual exclusion reaches $\Lambda_H^{\rm VV}$, $\Lambda_H^{\rm RR}$, $\Lambda_H^{\rm LL}$, $\Lambda_H^{\rm LR}$, $\Lambda_H^{\rm RL}$ and $\Lambda_H^{\rm TeV}$. Finally, the *identification reach* on the ADD scenario corresponds to the *minimum* of the *exclusion reaches*, $\Lambda_H^{\rm ID} = min\{\Lambda_H^{VV}, \Lambda_H^{AA}, \Lambda_H^{RR}, \Lambda_H^{LL}, \Lambda_H^{LR}, \Lambda_H^{RL}, \Lambda_H^{TeV}\}$. Clearly, for $\Lambda_H < \Lambda_H^{\rm ID}$ all composite-like CI models as well as the TeV^{-1} gravity model can be excluded as explanations of the deviation

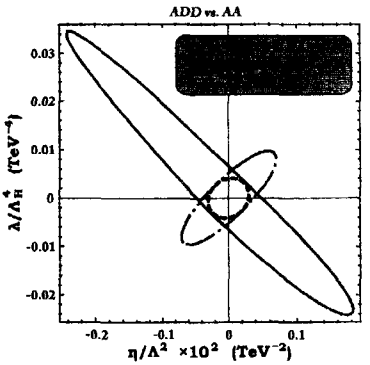

FIG. 1: $\Lambda_{\rm H}$ *vs.* $\Lambda_{\rm AA}$ confusion region from $e^+e^- \to e^+e^-$ at $\sqrt{s} = 0.5\,\text{TeV}$ and $\mathcal{L}_{\rm int} = 100\,\text{fb}^{-1}$.

or, equivalently, the ADD model can be identified. This simple χ^2 procedure can be applied in turn to all the individual sources of corrections to the SM in Eqs. (3) and (4), and the expected identification reaches on the corresponding Λ mass parameters can be determined analogously. The numerical results for the expected identification reaches are shown in Table 2 and Figs. 2–3. In Table 2, the blank entries refer to models for which the identification reach is found to fall below the current limits.

Table 2. 95% C.L. identification reaches (in TeV) at $\sqrt{s} = 1$ TeV and $\mathcal{L}_{\rm int} = 1000\ fb^{-1}$. Left and right entries refer to the polarization configurations $(|P^+|,|P^-|)$=(0,0) and (0.8, 0.6).

Model	Process			
	$e^+e^- \to e^+e^-$	$e^+e^- \to l^+l^-$	$e^+e^- \to \bar{b}b$	$e^+e^- \to \bar{c}c$
Λ_H	5.6; 6.9	5.9; 6.3	6.5; 6.9	5.8; 6.4
Λ^{ef}_{VV}	62.0; 98.6	142.2; 158.5	36.5; 157.5	136.1; 156.3
Λ^{ef}_{AA}	92.7; 142.9	153.1; 171.3	36.9; 161.7	155.8; 184.2
Λ^{ef}_{LL}	—; 104.0	—; 136.2	—; 152.2	—; 143.4
Λ^{ef}_{RR}	—; 106.1	—; 141.0	—; 151.6	—; 146.8
Λ^{ef}_{LR}	71.9; 115.8	—; 142.5	—; 121.6	—; 117.6
Λ^{ef}_{RL}	$\Lambda^{ef}_{RL} = \Lambda^{ef}_{LR}$	—; 144.3	—; 141.1	—; 132.8
M_C	9.7; 15.6	21.7; 35.3	11.0; 19.0	14.4; 20.4

3. Concluding remarks

In the previous section we have considered the problem of distinguishing the New Physics scenarios represented by the contactlike effective Lagrangians (2)-(4) from one another at the ILC, by analyzing polarized differential cross sections for fermion-pair production processes.

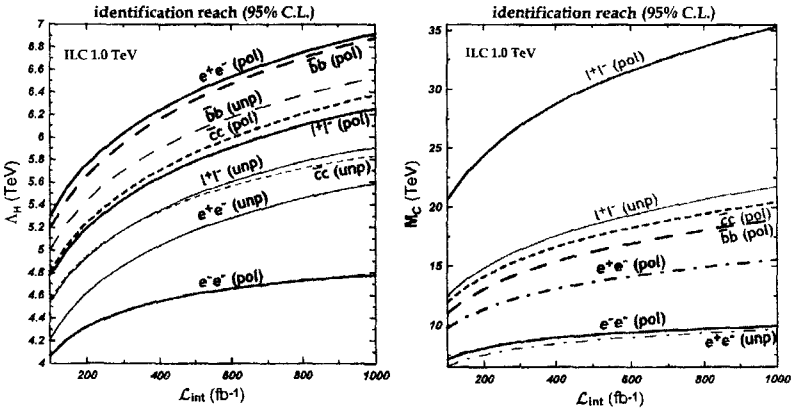

FIG. 2. Identification reach on the mass scale Λ_H (left panel) and compactification scale M_C (right panel) *vs.* integrated luminosity at $\sqrt{s} = 1\,\text{TeV}$.

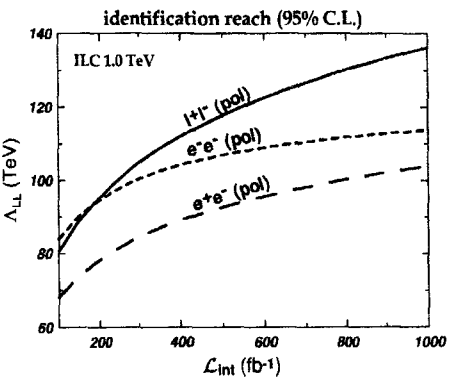

FIG. 3: Identification reach on the mass scale Λ_{LL} *vs.* integrated luminosity at $\sqrt{s} = 1\,\text{TeV}$.

The discovery reaches as well as the identification reaches are rather high compared to the current bounds, depending on energy and luminosity. The rôle of polarization in the various cases is shown by Figs. 1-3 and Table 2. It has an appreciable rôle in enhancing the identification sensitivity to the ADD model (Fig. 1). The enhancement is dramatic for models (3) and (4). Actually, as indicated by the blank entries in Table 2, polarization should be essential for the identification of some of the contact interaction scenarios (4), which would not be possible with unpolarized beams.

Acknowledgment

We would like to thank Prof. N. Paver for the enjoyable collaboration on the subject matter covered here.

References

[1] A. A. Pankov, N. Paver and A. V. Tsytrinov, Phys. Rev. D **73**, 115005 (2006).
[2] A. A. Pankov and N. Paver, Phys. Rev. D **72**, 035012 (2005).
[3] P. Osland, A. A. Pankov and N. Paver, Phys. Rev. D **68**, 015007 (2003).
[4] A. A. Pankov and N. Paver, Eur. Phys. J. C **29**, 313 (2003).
[5] G. Moortgat-Pick *et al.*, arXiv:hep-ph/0507011.
[6] N. Arkani-Hamed, S. Dimopoulos and G. R. Dvali, Phys. Lett. B **429**, 263 (1998).
[7] N. Arkani-Hamed, S. Dimopoulos and G. R. Dvali, Phys. Rev. D **59**, 086004 (1999).
[8] I. Antoniadis, N. Arkani-Hamed, S. Dimopoulos and G. R. Dvali, Phys. Lett. B **436**, 257 (1998).
[9] G. F. Giudice, R. Rattazzi and J. D. Wells, Nucl. Phys. B **544**, 3 (1999).
[10] T. Han, J. D. Lykken and R. J. Zhang, Phys. Rev. D **59**, 105006 (1999).
[11] J. L. Hewett, Phys. Rev. Lett. **82**, 4765 (1999).
[12] K. M. Cheung and G. Landsberg, Phys. Rev. D **65**, 076003 (2002).
[13] T. G. Rizzo and J. D. Wells, Phys. Rev. D **61**, 016007 (2000).
[14] E. Eichten, K. D. Lane and M. E. Peskin, Phys. Rev. Lett. **50**, 811 (1983).
[15] R. Rückl, Phys. Lett. B **129**, 363 (1983).
[16] For a review see, e.g., K. Cheung, arXiv:hep-ph/0409028.
[17] S. Eidelman *et al.* [Particle Data Group], Phys. Lett. B **502**, 1 (2004).